# Folding behaviors of two-dimensional flexible polymers ⊘

Jia-Qi Xu (iD) ; Rui Shi (iD) ; You-Liang Zhu ✉ (iD) ; Zhong-Yuan Lu (iD)

Check for updates

View Online

Export Citation

## Articles You May Be Interested In

Computer simulations of self-avoiding polymerized membranes

*J. Chem. Phys.* (April 1998)

# Folding behaviors of two-dimensional flexible polymers

View Online     Export Citation     CrossMark

Jia-Qi Xu,  [ID]   Rui Shi,[a]  [ID]   You-Liang Zhu,[b]  [ID]   and Zhong-Yuan Lu[c]  [ID]

## AFFILIATIONS

State Key Laboratory of Supramolecular Structure and Materials, College of Chemistry, Jilin University, Changchun 130023, China

[a] shirui816@gmail.com
[b] **Author to whom correspondence should be addressed:** youliangzhu@jlu.edu.cn
[c] luzhy@jlu.edu.cn

## ABSTRACT

Unlike one-dimensional polymers, the theoretical framework on the behaviors of two-dimensional (2D) polymers is far from completeness. In this study, we model single-layer flexible 2D polymers of different sizes and examine their scaling behaviors in solution, represented by $R_g \sim L^\nu$, where $R_g$ is the radius of gyration and $L$ is the side length of a 2D polymer. We find that the scaling exponent $\nu$ is 0.96 for a good solvent and 0.64 for under poor solvent condition. Interestingly, we observe a previously unnoticed phenomenon: under intermediate solvent conditions, the 2D polymer folds to maintain a flat structure, and as $L$ becomes larger, multiple folded structures emerge. We introduce a shape parameter $Q$ to diagram the relationship of folded structures with the polymer size and solvent condition. Theoretically, we explain the folding transitions by the competition between bending and solvophobic free energies.

*Published under an exclusive license by AIP Publishing.* https://doi.org/10.1063/5.0233042

Theoretical studies[1,2] and experimental observations[3,4] suggested that the behaviors and structures of sheet-like macromolecules, also known as two-dimensional (2D) polymers, differ significantly from linear polymers. However, the scaling behaviors along with configurational variation of 2D polymers under different solvent conditions are still ambiguous. As early as in the 1980s, lots of research[5–10] was conducted on the configuration of tethered membranes, i.e., the natural model of 2D polymers, sparking intensive debates regarding the existence of a crumpled structure. With no consideration on chain self-avoidance, Kantor *et al.* observed the elastic interactions at large distances driven by entropy, which subsequently result in an increase in the radius of gyration ($R_g$) following a scaling law of $(\ln L)^{1/2}$, where $L$ denotes the side length of the 2D polymers. When considering self-avoidance, the 2D polymers show a crumpled structure with $R_g \sim L^\nu$, where $\nu = 0.8 \pm 0.05$, in agreement with the finding derived from Flory theory.[11,12] In addition, the effect of finite bending stiffness $\kappa'$ on self-avoiding flexible 2D polymers was examined, unveiling a crumpled transition at low $\kappa'$. While for high $\kappa'$, the 2D polymer always maintains a flat structure.[13,14] On the contrary, Boal and co-workers claimed no crumpled structure was found in the simulations of 2D polymers with the model of hexagonally coordinated structures at both finite and infinite temperatures. The smallest eigenvalue of the radius of

the gyration tensor is described by $\lambda_3 \sim L^{\nu_3}$ with $\nu_3 \approx 0.65$, while the other two larger eigenvalues exhibit a linear relationship with $L$ as $\lambda \sim L$. Thus, in the thermodynamic limit $L \to \infty$, the 2D polymer would be roughly flat.[15,16] Abraham *et al.* explored a model that incorporated repulsive interactions between non-adjacent particles. They found that the 2D polymers are flat, even without the presence of bending stiffness.[17] In addition to flat and crumpled structures, the folded structures of 2D polymers are discovered to indicate a diversity of configurations.[18] Upon recent advancements in nanotechnology, the 2D polymers are becoming a central topic in materials science.[19–25] The experimentally observed folded structure was realized by monolayer graphene oxide (GO). It was discovered that GO sheets form a simple folded structure to minimize solvation energy.[26] By varying the concentration of GO in solution and adjusting the solution properties, the conformational transition of the monolayer GO was manipulated.[27,28] This was further confirmed by molecular dynamics simulations, which provided insights into the scaling relationship. Factors such as the size and bending stiffness of the 2D polymer, along with the solvent effect on surface interactions, contribute to the transition from a flat to a folded structure.[29] Xu *et al.* applied machine learning techniques to analyze the roles of factors such as metric changes, curvature, conformational anisotropy and surface contact in the morphology formation of flat, folded,

and crumpled structures. It was also theoretically demonstrated that the occurrence of folding and the number of folds is related to the Föppl–von Kármán number and the shrinkage ratio.[30,31]

Previous simulation studies employed the models with implicit solvents, where the solvent conditions were incorporated in the interactions between the units of 2D polymers. Here, we report simulation results using the dissipative particle dynamics method with the explicit solvent.[32] In particular, we construct a flexible 2D polymer model with coarse-grained P (colored in cyan) beads in a square network with $L$ beads along each edge, for a total of $N = L^2$ beads, as shown in Fig. 1. The simulation box is filled with solvent beads S (colored in tangerine) and the number density $\rho$ is 3. The repulsive interactions between the same beads are set as $\alpha_{PP} = \alpha_{SS} = 25$. We vary $\alpha_{PS}$ from 25 to larger values representing different solvent conditions.

The radius of gyration is used to describe the size of 2D polymers,[33,34]

$$R_g^2 = \frac{1}{N^2} \left\langle \sum_{i,j=1}^{N} (r_i - r_j)^2 \right\rangle. \tag{1}$$

The angular brackets denote an average of many independent configurations.

The $\alpha_{PS} = 25$ yields an asymptotically flat network structure, while a collapsed spherical structure is observed when $\alpha_{PS} = 35$. At intermediate parameters, such as $\alpha_{PS} = 29$, the folded structure is dominant in the system. In previous studies, collapsed structures were observed in the absence of angle bending potential.[25] Our findings suggest that the flexible model of 2D polymer without bending potential still exhibits a flat structure in good solvents, highlighting the crucial role of the solvent environment on shaping the behaviors of 2D polymers.

Figure 2 shows $R_g$ as a function of $L$ in cases of different $\alpha_{PS}$. With the same $L$, $R_g$ decreases as $\alpha_{PS}$ increases. This behavior can be attributed to the increased solvophobic interaction that is equivalent to the increased intramembrane affinity between the polymer beads, causing the membrane to collapse into a compact structure. When $\alpha_{PS} = 25$, 26, and 27 (i.e., good solvent condition), the scaling exponent $\nu$ in $R_g \sim L^\nu$ is $0.96 \pm 0.01$ [Fig. S1(a)]. The scaling exponent is slightly smaller than the theoretically predicted value of 1.0. The


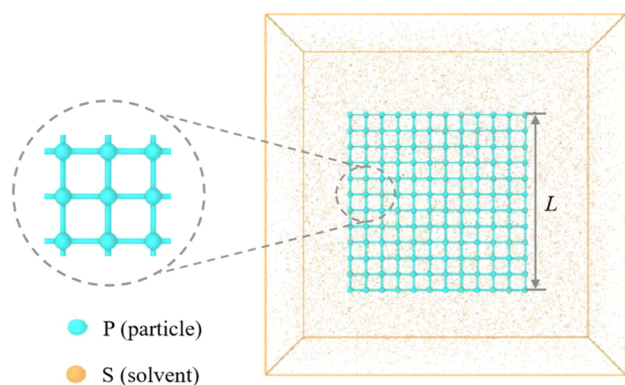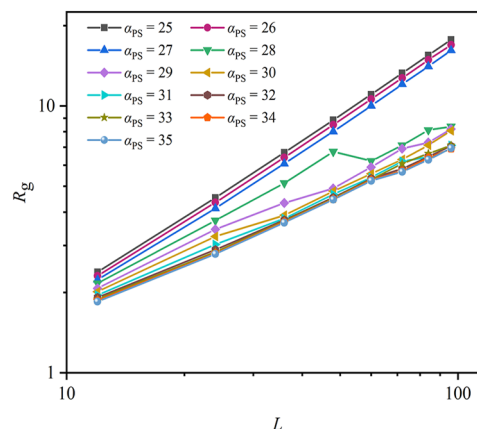
**FIG. 2.** Log–log plot of the relationship between the radius of gyration $R_g$ and the size of the 2D polymer $L$ under different solvent conditions.

equilibrium structure is flat, as shown in Fig. 3(b). When $\alpha_{PS} = 31$, 32, 33, 34, and 35 (i.e., poor solvent condition), the scaling exponent is $0.64 \pm 0.01$ [Fig. S1(b)] close to the theoretically predicted value of 2/3, and the equilibrium structure is a collapsed sphere, as shown in Fig. 3(g).

When $\alpha_{PS}$ takes the value of 28, 29, and 30 for the intermediate solvent condition, structural transitions occur as $L$ increases, resulting in the shifts of scaling exponent. As shown in Fig. 2, there are two distinct transitions of scaling behavior with $\alpha_{PS} = 29$, occurring at $L = 36$ and 72, respectively. Each transition of the scaling exponent corresponds to a transformation of the 2D polymer structure. For instance, the equilibrium structure preceding the first transition point corresponds to that shown in Fig. 3(c) with $\nu = 0.73$, the equilibrium structure between the first and the second transition points corresponds to that shown in Fig. 3(d) with $\nu = 0.85$, and the structure following the second transition point corresponds to that shown in Fig. 3(e) with $\nu = 0.86$. Different from the previous work, where only one shift of the scaling exponent was observed upon increasing angle force constants,[25] we observe two clear transitions that can be attributed to the much larger size of 2D polymers modeled in our simulations. To profile the structural changes, we analyze the distribution of the radius of gyration. Notably, two distinct peaks appear on the distribution of radius of gyration when $L = 36$ and 78, as shown in Figs. S2(a) and S2(b). This means that as the size of the 2D polymer approaches the transition point, we can observe the coexistence of two different structures. Moreover, the position of the first transition point tends to occur at smaller $L$ as $\alpha_{PS}$ increases, while the position of the second transition point also shifts to smaller $L$. We speculate that as $L$ continues to increase, the 2D polymers will continue to fold. As shown in Fig. 2, the important stage of scaling transition is between $\alpha_{PS} = 27$ and $\alpha_{PS} = 28$. When $\alpha_{PS}$ ranges from 27.1 to 27.5, we calculate the relationship between the radius of gyration of 2D polymers and their size, as well as the relationship between the eigenvalues of the radius of the gyration tensor and the size of 2D polymers, as shown in Fig. S3. The results indicate that the dominant structure of the 2D polymer within this range of solvent conditions remains a folded structure.
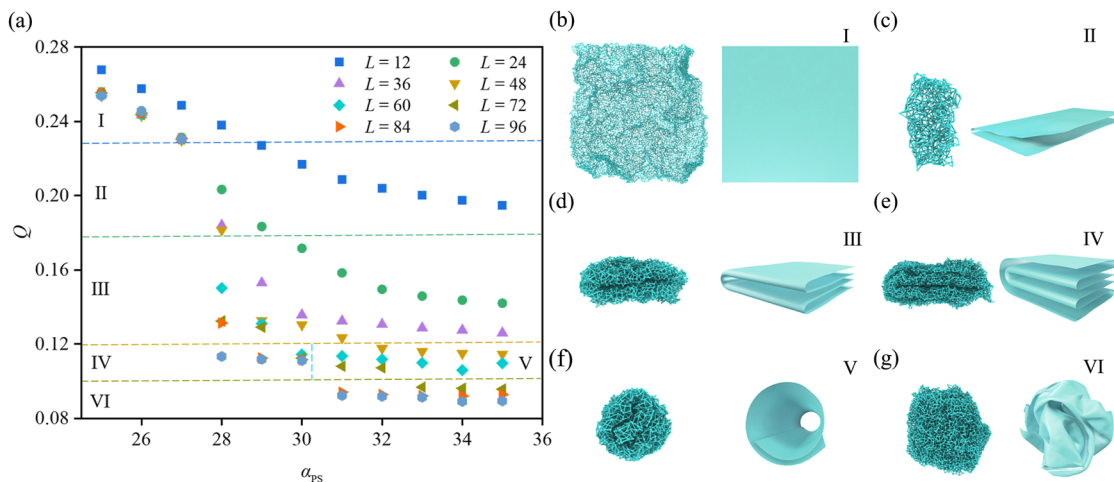


**FIG. 1.** Initial structure of $L = 12$ 2D polymer; $L$ is defined as the number of P beads on one side.

**FIG. 3.** (a) Relationship between the shape parameter $Q$ and the solvent condition $\alpha_{PS}$ when the size of the 2D polymer is different. (b) $\alpha_{PS} = 25$, snapshot and schematic structure of a 2D polymer with size $L = 96$. (c)–(e) $\alpha_{PS} = 29$, snapshots and schematic structures showcasing 2D polymers with sizes $L = 24$, 72, and 96 in equilibrium states, respectively. (f) and (g) $\alpha_{PS} = 35$, snapshots and schematic structures for 2D polymers with $L = 60$ and 96, respectively.

To characterize the structure, we calculate the eigenvalues of the radius of gyration tensor,[35,36]

$$T = \begin{bmatrix} S_{xx} & S_{xy} & S_{xz} \\ S_{yx} & S_{yy} & S_{yz} \\ S_{zx} & S_{zy} & S_{zz} \end{bmatrix}, \tag{2}$$

with $S_{ab} = \frac{1}{N}\sum_{i=1}^{N}(a_i - a_{cm})(b_i - b_{cm})$ with $a, b = x, y, z$. Here, $N$ is the total number of P beads in the 2D polymer model, $a_i$ is the position of the $i$th bead, and $a_{cm}$ is the coordinate of the centroid of the 2D polymer in the $a$ direction. By diagonalizing the matrix T, three eigenvalues, $\lambda_1$, $\lambda_2$, and $\lambda_3$, can be obtained with $\lambda_1 > \lambda_2 > \lambda_3$. Prior to the first transition point, $\lambda_1$ is approximately twice $\lambda_2$, indicating a primary folded configuration, as shown in Fig. 3(c). After the first transition point but before the second, $\lambda_1 \approx \lambda_2$, indicating a structural change to a secondary folded configuration, as shown in Fig. 3(d). Subsequent to the second transition point, $2\lambda_1 \approx 3\lambda_2$, signifying another structural change to a tertiary folded configuration, as shown in Fig. 3(e). As the number of folded layers increases, the stiffness of the structure becomes larger, which may eventually prevent further folding beyond a certain number of layers, analogous to the concept of origami, where a thin piece of paper with limited thickness can only be folded a certain number of times.

To categorize various folding structures of 2D polymers, we introduce a customized shape parameter $Q$, defined as $Q = (\lambda_1 + \lambda_2)/L$. We perform systematic simulations to summarize how solvent conditions $\alpha_{PS}$ affect the 2D polymer shape and build up a phase diagram based on $Q$. As shown in Fig. 3(a), the 2D polymer structures can be classified into six classes. When $Q \leq 0.1$ (class VI), the 2D polymer adopts a collapsed structure, as shown in Fig. 3(g). When $0.1 < Q \leq 0.12$ and for $\alpha_{PS} \leq 30$ (class IV), the 2D polymer is a tertiary folded structure, as shown in Fig. 3(e), and for $\alpha_{PS} > 30$ (class V), the 2D polymer possesses a cylinder structure, as shown in Fig. 3(f). When $0.12 < Q \leq 0.18$ (class III), the 2D polymer has

a secondary folded structure, as shown in Fig. 3(d). This structure aligns with the folded structure reported in previous studies.[29] When $0.18 < Q \leq 0.23$ (class II), the 2D polymer has a primary folded structure, as shown in Fig. 3(c). Finally, for $Q > 0.23$ (class I), the 2D polymer is an asymptotically flat structure, as shown in Fig. 3(b). It should be noted that the categorization of these classes is devised to clarify visual observations.

To explain the folding transition of 2D polymers under various solvent conditions, we use a theoretical model describing the competition between the 2D polymer bending energy and solvent repulsion energy, which potentially drives it to form a folding structure. This is consistent with recent research on scaling relations for 2D polymers. Our findings further reinforce the idea that solvent conditions play a crucial role in determining the conformational behavior of 2D polymers. As demonstrated in both simulations and experiments, 2D polymers transition from a flat structure to a folding structure depending on the solvent condition.[27,29] The surface energy, represented as

$$F_{surf} = -\gamma A, \tag{3}$$

incorporates $\gamma$ as the surface tension and $A$ as the total surface area of the folding 2D polymer. In the context of the folded states, such as the tertiary folded structure shown in Fig. 3(e), the polymer's dimensions can be envisioned as a cuboid with three orthogonal axes ($\hat{l}_1$, $\hat{l}_2$, and $\hat{l}_3$), i.e., the three eigenvectors of the gyration tensor. We calculate the bending energy as

$$F_{bend} = \kappa \int_A \widehat{n} \cdot \hat{l}_3 dx, \tag{4}$$

where $\kappa$ denotes the bending energy constant, and $\widehat{n}$ and $\hat{l}$ symbolize the normal of a patch on the 2D polymer and normal of the polymer as a whole, essentially, the axis of least gyration, respectively. The bending constant $\kappa$ is inherently correlated to the thickness of the

folded structure. Assuming an n-folded structure and the thickness to be $l_3$, with a slight bend angle $\theta$ in relation to $\hat{l}_3$, an estimation of the bending energy is

$$F_{bend} = \kappa\theta^2 = \int_{R\theta}^{(R+l_3)\theta} k(l - R\theta)^2 dl = \frac{1}{3}kl_3^3\theta^3. \quad (5)$$

In Eq. (5), we assume that the bending surface is cylindrical with a radius $R$, and $k$ represents the stretching constant of the 2D polymer. Consequently, $R\theta$ and $(R + l_3)\theta$ denote the perimeters of the inner and outer bending surfaces, respectively. We further assume that the inner surface is 'relaxed', implying that the bending energy $F_{bend}$ arises primarily from the stretching of the layers. Given the folded structures, the flat surface bend angle is minimal across all states, $\theta$ can be omitted, and therefore, $\kappa \sim l_3^3$ can be derived. Here, $l_1 l_2 l_3 = A_0 b$, with $b$ being the monomer size. We simply set $b = 1$ as the length unit in our work, hence $F_{bend} \sim kA_0 l_3^2$. The total surface area $A$ of a cuboid with orthogonal axes $l_1$, $l_2$, and $l_3$ is estimated as

$$A = 2l_1 l_2 + 4\sqrt{l_1 l_2}l_3. \quad (6)$$

In the simulations, as $\alpha_{PS}$ increases, the surface tension increases rapidly, prompting the 2D polymer to fold. Therefore, for a polymer folded n times, the (n + 1)th fold only materializes when the surface hydrophobicity strength surpasses the current nth folding state's bending energy gain. This assumption can be represented as

$$\frac{k}{\gamma}\left(A_0 l_3^2 \times \left(\beta^3 - 1\right)\right) = 2l_1 l_2 + 4\sqrt{l_1 l_2}l_3 - \frac{2l_1 l_2}{\beta} - 4\beta l_3\sqrt{\frac{l_1 l_2}{\beta}}. \quad (7)$$

In Eq. (7), we introduce the folding parameter $\beta$, with $\beta = A_0/A$. For folding in half, also known as V-fold, i.e., the primary folded and secondary folded structures shown in Figs. 3(c) and 3(d), respectively, the folding parameter is $\beta_V = 2$. Our simulations also reveal an alternative folding class, i.e., the NV-fold [tertiary folded in Fig. 3(e)], corresponding to the folding parameter $\beta_{NV} = 1.83$. The simulation results are incorporated into the theoretical model derived above, we can plot the phase diagram shown in Fig. 4. The phase diagram illustrates the classification of folding types and shows how the system evolves as $\alpha_{PS}$ increases and the ratio $k/\gamma$ decreases. This results in thicker folded structures and a rightward shift in the phase boundaries. In Fig. 4, solid lines, fitted using Eq. (7), delineate the boundaries between different folding classes. The square and triangle symbols indicate conditions at $\alpha_{PS} = 27.5$ and $\alpha_{PS} = 28$, respectively, and V-folds are the dominant structures. Circle and diamond symbols represent V-fold and NV-fold classes, respectively, both at $\alpha_{PS} = 29$. This is because as hydrophobicity increases and induces compressive forces, the 2D polymer adapts by selecting pathways that minimize hydrophobic changes during successive foldings, effectively reducing $\beta$. This adaptation leads to the emergence of an NV-fold structure at $\alpha_{PS} = 29$. Based on the phase diagram, the folded structure of the 2D polymer can be predicted.

In conclusion, we employ the model of flexible 2D polymers with an explicit solvent and depict a class of structures, including flat, cylindrical, and folded structures under different solvent conditions.
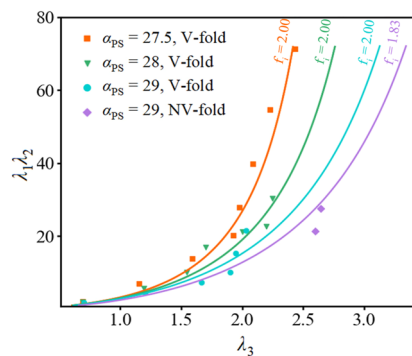


**FIG. 4.** Fitting relationship between the V-folded structure and the NV-folded structure when $\alpha_{PS} = 27.5$, 28, and 29.

For a good solvent, the scaling exponent $\nu = 0.96 \pm 0.01$ with flat morphologies is slightly smaller than theoretically expected value. For a poor solvent, the $\nu = 0.64 \pm 0.01$ with collapsed morphologies is very close to the theoretical prediction. Under intermediate solvent conditions, there are obvious turning points in the scaling exponent, along with the transformation of folded structures, instead of crumpled structures. We define the shape parameter $Q$ and classify the equilibrium structures of 2D polymers into different categories. By establishing a correlation between the bending energy and the solvent repulsive energy, our theoretical analysis rationalizes the presence of folded structures.

The supplementary material encompasses the details of simulation methods, the scaling index of 2D polymers under different solvent conditions, the frequency distribution of the radius of gyration under different sizes, and the relationship between the eigenvalues of the radius of gyration and the size of 2D polymers under different solvent conditions.

## AUTHOR DECLARATIONS

### Conflict of Interest

The authors have no conflicts to disclose.

### Author Contributions

**Jia-Qi Xu**: Data curation (equal); Investigation (equal); Writing – original draft (equal). **Rui Shi**: Data curation (equal); Investigation (equal). **You-Liang Zhu**: Software (equal); Supervision (equal); Writing – review & editing (equal). **Zhong-Yuan Lu**: Supervision (equal); Writing – review & editing (equal).

## DATA AVAILABILITY

The data that support the findings of this study are available from the corresponding authors upon reasonable request.

## REFERENCES

[1] M. Rubinstein, R. H. Colby *et al.*, *Polymer Physics* (Oxford University Press, New York, 2003), Vol. 23.

[2] D. Nelson, T. Piran, and S. Weinberg, *Statistical Mechanics of Membranes and Surfaces* (World Scientific, 2004).

[3] T. Hwa, E. Kokufuta, and T. Tanaka, "Conformation of graphite oxide membranes in solution," Phys. Rev. A **44**, R2235 (1991).

[4] M. S. Spector, E. Naranjo, S. Chiruvolu, and J. A. Zasadzinski, "Conformations of a tethered membrane: Crumpling in graphitic oxide?," Phys. Rev. Lett. **73**, 2867 (1994).

[5] L. Radzihovsky and J. Toner, "A new phase of tethered membranes: Tubules," Phys. Rev. Lett. **75**, 4752 (1995).

[6] M. Paczuski, M. Kardar, and D. R. Nelson, "Landau theory of the crumpling transition," Phys. Rev. Lett. **60**, 2638 (1988).

[7] D. Liu and M. Plischke, "Monte Carlo studies of tethered membranes with attractive interactions," Phys. Rev. A **45**, 7139 (1992).

[8] Y. Kantor and K. Kremer, "Excluded-volume interactions in tethered membranes," Phys. Rev. E **48**, 2490 (1993).

[9] A. D. Schlüter, P. Payamyar, and H. C. Öttinger, "How the world changes by going from one- to two-dimensional polymers in solution," Macromol. Rapid Commun. **37**, 1638 (2016).

[10] M. Bowick, M. Falcioni, and G. Thorleifsson, "Numerical observation of a tubular phase in anisotropic membranes," Phys. Rev. Lett. **79**, 885 (1997).

[11] Y. Kantor, M. Kardar, and D. R. Nelson, "Tethered surfaces: Statics and dynamics," Phys. Rev. A **35**, 3056 (1987).

[12] Y. Kantor, M. Kardar, and D. R. Nelson, "Statistical mechanics of tethered surfaces," Phys. Rev. Lett. **57**, 791 (1986).

[13] Y. Kantor and D. R. Nelson, "Phase transitions in flexible polymeric surfaces," Phys. Rev. A **36**, 4020 (1987).

[14] Y. Kantor and D. R. Nelson, "Crumpling transition in polymerized membranes," Phys. Rev. Lett. **58**, 2774 (1987).

[15] M. Plischke and D. Boal, "Absence of a crumpling transition in strongly self-avoiding tethered membranes," Phys. Rev. A **38**, 4943 (1988).

[16] D. Boal, E. Levinson, D. Liu, and M. Plischke, "Anisotropic scaling of tethered self-avoiding membranes," Phys. Rev. A **40**, 3292 (1989).

[17] F. F. Abraham, W. E. Rudge, and M. Plischke, "Molecular dynamics of tethered membranes," Phys. Rev. Lett. **62**, 1757 (1989).

[18] F. F. Abraham and M. Kardar, "Folding and unbinding transitions in tethered membranes," Science **252**, 419 (1991).

[19] J. Sakamoto, J. van Heijst, O. Lukin, and A. D. Schlüter, "Two-dimensional polymers: Just a dream of synthetic chemists?," Angew. Chem., Int. Ed. **48**, 1030 (2009).

[20] P. Payamyar, B. T. King, H. C. Öttinger, and A. D. Schlüter, "Two-dimensional polymers: Concepts and perspectives," Chem. Commun. **52**, 18 (2016).

[21] R. B. Pandey, K. L. Anderson, and B. L. Farmer, "Multiscale mode dynamics of a tethered membrane," Phys. Rev. E **75**, 061913 (2007).

[22] R. B. Pandey, K. L. Anderson, and B. L. Farmer, "Multiscale dynamics of an interacting sheet by a bond-fluctuating Monte Carlo simulation," J. Polym. Sci., Part B: Polym. Phys. **44**, 2512 (2006).

[23] R. B. Pandey, K. L. Anderson, H. Heinz, and B. L. Farmer, "Conformation and dynamics of a self-avoiding sheet: Bond-fluctuation computer simulation," J. Polym. Sci., Part B: Polym. Phys. **43**, 1041 (2005).

[24] R. B. Pandey, K. L. Anderson, and B. L. Farmer, "Effect of temperature and solvent on the structure and transport of a tethered membrane: Monte Carlo simulation," J. Polym. Sci., Part B: Polym. Phys. **43**, 3478 (2005).

[25] S. T. Knauert, J. F. Douglas, and F. W. Starr, "Morphology and transport properties of two-dimensional sheet polymers," Macromolecules **43**, 3438 (2010).

[26] A. R. Koltonow, C. Luo, J. Luo, and J. Huang, "Graphene oxide sheets in solvents: To crumple or not to crumple?," ACS Omega **2**, 8005 (2017).

[27] Y. Wang, S. Wang, P. Li, S. Rajendran, Z. Xu, S. Liu, F. Guo, Y. He, Z. Li, Z. Xu, and C. Gao, "Conformational phase map of two-dimensional macromolecular graphene oxide in solution," Matter **3**, 230 (2020).

[28] Y. Jiang, Y. Wang, Z. Xu, and C. Gao, "Conformation engineering of two-dimensional macromolecules: A case study with graphene oxide," Acc. Mater. Res. **1**, 175 (2020).

[29] P. Li, S. Wang, F. Meng, Y. Wang, F. Guo, S. Rajendran, C. Gao, Z. Xu, and Z. Xu, "Conformational scaling relations of two-dimensional macromolecular graphene oxide in solution," Macromolecules **53**, 10421 (2020).

[30] Y. Zhao, J. Qin, S. Wang, and Z. Xu, "Unraveling the morphological complexity of two-dimensional macromolecules," Patterns **3**, 100497 (2022).

[31] Y. Wang, S. Wang, Y. Gao, P. Li, B. Zhao, S. Liu, J. Ma, L. Wang, Q. Yin, Z. Wang *et al.*, "Determinative scrolling and folding of membranes through shrinking channels," Sci. Adv. **10**, eadm7737 (2024).

[32] R. D. Groot and P. B. Warren, "Dissipative particle dynamics: Bridging the gap between atomistic and mesoscopic simulation," J. Chem. Phys. **107**, 4423 (1997).

[33] M. Doi, S. F. Edwards, and S. F. Edwards, *The Theory of Polymer Dynamics* (Oxford University Press, 1988), Vol. 73.

[34] P.-G. De Gennes, *Scaling Concepts in Polymer Physics* (Cornell University Press, 1979).

[35] B. Li, Y.-L. Zhu, H. Liu, and Z.-Y. Lu, "Brownian dynamics simulation study on the self-assembly of incompatible star-like block copolymers in dilute solution," Phys. Chem. Chem. Phys. **14**, 4964 (2012).

[36] J. Rudnick and G. Gaspari, "The asphericity of random walks," J. Phys. A Math. Gen. **19**, L191 (1986).

18 February 2025 21:07:58